ELSEVIER

Biochemical Pharmacology 63 (2002) 455–462

Biochemical Pharmacology

Anti-cancer action of 4-iodo-3-nitrobenzamide in combination with buthionine sulfoximine: inactivation of poly(ADP-ribose) polymerase and tumor glycolysis and the appearance of a poly(ADP-ribose) polymerase protease

Pal I. Bauer[a,b,1], Jerome Mendeleyeva[a], Eva Kirsten[a,b], John A. Comstock[a,2], Alaeddin Hakam[a,b], Kalman G. Buki[a,3], Ernest Kun[a,b,*]

[a]*Laboratory for Environmental Toxicology and Chemistry, Octamer Inc., Octamer Research Foundation, Romberg Tiburon Centers, San Francisco State University, Tiburon, CA 94920, USA*
[b]*Department of Anatomy and Cellular and Pharmacology, School of Medicine, University of California, San Francisco, CA 94143-0452, USA*

Received 19 December 2000; accepted 19 June 2001

Abstract

E-ras 20 tumorigenic malignant cells and CV-1 non-tumorigenic cells were treated with a drug combination of 4-iodo-3-nitrobenzamide (INO_2BA) and buthionine sulfoximine (BSO). Growth inhibition of E-ras 20 cells by INO_2BA was augmented 4-fold when cellular GSH content was diminished by BSO, but the growth rate of CV-1 cells was not affected by the drug combination. Analyses of the intracellular fate of the prodrug INO_2BA revealed that in E-ras 20 cells about 50% of the intracellular reduced drug was covalently protein-bound, and this binding was dependent upon BSO, whereas in CV-1 cells BSO did not influence protein binding. Glyceraldehyde-3-phosphate dehydrogenase (GAPDH) was identified as the protein that covalently binds the reduction product of INO_2BA, which is 4-iodo-3-nitrosobenzamide. Since only the enzymatically reduced drug INOBA bound covalently to GAPDH, the BSO-dependent covalent protein–drug association indicated an apparent nitro-reductase activity present in E-ras 20 cells, but not in CV-1 cells, explaining the selective toxicity. Covalent binding of INOBA to GAPDH inactivated this enzyme *in vitro*; INO_2BA + BSO also inactivated cellular glycolysis in E-ras 20 cells because it provided the precursor to the inhibitory species: INOBA. Another event that occurred in INO_2BA + BSO-treated E-ras 20 cells was the progressive appearance of a poly(ADP-ribose) polymerase protease. This enzyme was partially purified and characterized by the polypeptide degradation product generated from PARP I, which exhibited a 50 kDa mass. This pattern of proteolysis of PARP I is consistent with a drug-induced necrotic cell killing pathway.

Keywords: 4-Iodo-3-nitrobenzamide reduction; Poly(ADP-ribose) polymerase protease induction; Inhibition of glycolysis; Selective tumor necrosis

1. Introduction

Poly(ADP-ribose) polymerase (PARP I) (EC 2.4.2.30) is a ubiquitous highly abundant (0.5×10^6 copies per cell, cf. [1]) non-histone nuclear protein that utilizes NAD^+ for the synthesis of covalently protein-bound ADP-ribose polymers. The biological significance of PARP I is still debated. One of the better-defined roles of PARP I is its function as a DNA nick-sensor [2,3]. In addition, a large number of diverse chromatin functions have also been correlated to PARP I, such as DNA-repair, sister chromatid exchange, and regulation of genomic integrity (for review, see [4]).

* Corresponding author. Tel.: +1-415-514-2145; fax: +1-415-388-7024.
E-mail address: ernestkun@mac.com (E. Kun).
[1] Present address: Department of Medical Biochemistry, Semmelweis University, Budapest, Hungary.
[2] Present address: Veterans Administration Medical Center, San Francisco, CA 94121, USA.
[3] Present address: Department of Anatomy, University of Turku, Turku, Finland.

Abbreviations: PARP I, poly(ADP-ribose) polymerase; INO_2BA, 4-iodo-3-nitrobenzamide; BSO, buthionine sulfoximine; INOBA, 4-iodo-3-nitrosobenzamide; GAPDH, glyceraldehyde-3-phosphate dehydrogenase; DMEM, Dulbecco's modified Eagle's medium; FBS, fetal bovine serum; PCA, perchloric acid.

0006-2952/02/$ – see front matter
PII: S0006-2952(01)00872-3

Most of the work concerned with the biologic role of PARP I has been done with subcellular systems. One of the significant tools for the study of the cellular importance of PARP I is the genetic deletion of PARP I in mouse models [5]. In a recent study, gene expression in normal and PARP $I^{-/-}$ primary fibroblasts was compared by the oligonucleotide microarray hybridization technique [6], and 91 gene expressions were reported to exhibit quantitative deviations in PARP $I^{-/-}$ cells (30% down-regulated and 69% augmented). Several of the protein products appear to be components of signal pathways, also modified by exposure of E-ras 20 cancer cells to reversible PARP I inhibitors [7–9], that inhibit tumor growth and reverse the malignant phenotype. Possible indirect effects due to protein interactions of PARP I at the RNA polymerase II level [10,11] or at the Topo I level [12,13] may complicate the discrimination between direct consequences of gene deletion and other regulatory systems that act on mechanisms of gene reading. The potential inaccuracy of predicting the *in vivo* consequences of gene deletion is illustrated by the *Myf*-5 gene that regulates muscle development, yet its deletion produces rib abnormalities [14].

We have attempted to investigate the pharmacologic consequences of functional PARP I deletion by inhibitory ligands, presumably inflicting acute cellular effects of PARP I inhibition. Obvious objections to this experimental approach are possible effects of ligands that appear not to be related to known functions of PARP I, a complication that can be diminished by the synthesis of more specific inhibitors and by the experimental analyses of drug-induced effects that may or may not be predicted consequences of PARP I inhibition, as reported here.

We developed both reversibly acting [7–9] and irreversible inhibitors of PARP I [15–18]. One of the most specific and effective reversible inhibitors, 5-iodo-6-amino-1, 2-benzopyrone [7], has proven to be active both *in vitro* and *in vivo* against peroxynitrite-induced tissue injuries [19,20] and endotoxin-elicited inflammatory responses [21] in addition to the inhibition of cancers [7–9]. An irreversible inactivation of PARP I was demonstrated for C-nitroso ligands of PARP I [15], which attack the asymmetric Zn^{2+} fingers of both PARP I and the HIV virus [16–18]. The pleiotropic effects of PARP I ligands have been reviewed, and mechanisms have been traced to both enzyme inhibition and to the binding of PARP I protein to various cellular sites [22].

In a preceding report [23], we described a significant tumoricidal effect in cell cultures with a combination of INO_2BA and BSO, a known inhibitor of GSH synthesis. The tumoricidal action of the combination of INO_2BA + BSO was effective in 13 human cancer cell lines [23]. We have chosen the tumor cell construct E-ras 20 [7] in our present work because it is by far the most tumorigenic cell type of the 13 human tumor cell lines [23] tested in nude mice xenografts. We proposed a reaction mechanism that consists of the reduction of the nitro group in INO_2BA to a nitroso group, indicating that INO_2BA serves as prodrug for 4-iodo-3-nitrosobenzamide (INOBA). Removal of GSH by BSO prevents further reduction [23]. The nitroso product induces Zn^{2+} ejection from the asymmetric Zn^{2+} fingers of PARP I [23] and inactivates PARP I. The significance of GSH in the metabolism of INO_2BA was demonstrated *in vivo* by the rapid reduction of the drug to the pharmacologically inactive amine [24] in livers of dogs and rats, as previously predicted [23].

We report here the robust tumoricidal action of the above drug combination and describe: (a) an apparent E-ras 20 cell selective action of the drug combination, (b) the covalent binding of enzymatically formed INOBA to the thiol group of GAPDH (EC 1.2.1.12) with coinciding inactivation of glycolysis, and (c) the appearance of a PARP I protease, which was defined by its partial purification and the demonstration of the main proteolytic polypeptide fragment (50 kDa) of PARP I.

2. Materials and methods

The cultures of E-ras 20 cells, a ras transformed bovine endothelial cell line, and the analytical methods used were the same as reported earlier [7]. The CV-1 cells, African green monkey normal kidney fibroblasts, were obtained from the American Type Culture Collection and were grown according to the protocol of the vendor.

The syntheses of ^{14}C-labeled INO_2BA and of INOBA from [^{14}C]-*p*-aminobenzoic acid were carried out following a published method [23] by L. Clizbe (SRI). The specific activity of the final products was 15 mCi/mmol.

Cellular uptake of [^{14}C]-INO_2BA was measured as previously reported [7]. Briefly, cell cultures were incubated with various concentrations of ^{14}C-labeled INO_2BA under conditions of logarithmic cell growth, and then were washed free of external ^{14}C-labeled drug with PBS containing the same concentration of unlabeled drug as used during the incubation. Intracellular drug concentration was assayed in detached cell suspensions by radiochemical analysis [7]. Equilibration of extra- and intracellular ^{14}C-labeled drug occurred in 18 hr, and it is for this reason that protein binding and the effect of BSO were determined at this time (see legend of Table 1).

Crystalline GAPDH and its antibody, as well as assay kits, were purchased from the Biodesigns and Sigma, respectively.

Glycolysis of E-ras 20 and CV-1 cells was monitored by a microphysiometer (Molecular Devices) as reported [7].

Isolation and sequencing of a decapeptide fragment of the 50 kDa PARP I proteolytic polypeptide were done by methods as reported previously [25], and the synthesis of T(N^{*}) KSEKRMLKLHHHHH polypeptide, which is part of the 50 kDa polypeptide formed by the drug-induced PARP I protease, was carried out by standard techniques by

Table 1
Uptake and protein binding of INO_2BA in E-ras 20 cells in the absence or presence of BSO

Extracellular added drug (μM)	Absence or presence of BSO (1 mM)	Intracellular total drug concentration (μM)	Intracellular protein-bound drug (μM)
27	No BSO	24.5 ± 3.5	10.5 ± 1.5
	BSO present	52 ± 8.0	35 ± 4
40	No BSO	39.5 ± 6.5	15 ± 3
	BSO present	82.2 ± 8.2	44 ± 4
53	No BSO	51.5 ± 6.5	28.5 ± 3.5
	BSO present	100 ± 15.6	58.5 ± 7.5

^{14}C-labeled INO_2BA (15 mCi/mmol) was added to the growth medium of preconfluent cultures in 9.6 cm wells at the concentrations noted above. BSO, where indicated, was added 1 hr prior to the addition of INO_2BA. The cultures were then incubated overnight (18 hr). After medium removal, the monolayers were washed four times with 1 mL PBS containing non-radioactive INO_2BA. For "intracellular total drug" assays, cells were lysed in 1 mL of 0.2 N NaOH, 4% Na_2CO_3, and radioactivity was determined by liquid scintillation counting. For "acid precipitable intracellular material", cells were suspended in 1 mL of 10% PCA, frozen at −20°, re-thawed, sonicated, and delivered onto glass fiber filters. Radioactivity was determined after extensive washing and drying of the filters. The cell volumes for each sample were assessed from similarly treated parallel wells, in which the cells were detached and counted by a haemocytometer. Results (means ± SD) of three experiments determined in triplicates are given as micromolar radioactive INO_2BA.

the Large Scale Biology Co. N* indicates that the L-isomer was replaced with the D-isomer. GSH was assayed by the procedure given by Biosyntech S.A. (Cedex).

3. Results

3.1. Effect of the drug combination on cell growth of E-ras 20 cells

As shown in Fig. 1, the presence of 0.5 mM BSO increased the growth-suppressing action of INO_2BA by 4–5-fold. GSH concentration in the presence of 0.5–1.0 mM BSO decreased from a 16 ± 5 mM ($N = 3$) concentration to below 4 μM. This effect was comparable to those reported with other cancer cells [23]. Comparison of the action of 0–128 μM INO_2BA + BSO was done at all drug levels. However, in the presence of BSO there was no cell growth above 32 μM INO_2BA; therefore, these data were omitted from Fig. 1.

3.2. Apparent E-ras 20 selectivity of the drug combination

As illustrated in Fig. 2, the slow rates of cell growth of CV-1 cells remained uninfluenced by the combination of INO_2BA + BSO (Fig. 2B), whereas the vigorous growth of E-ras 20 cells was suppressed dramatically after a 1-day exposure to the drug (Fig. 2A).

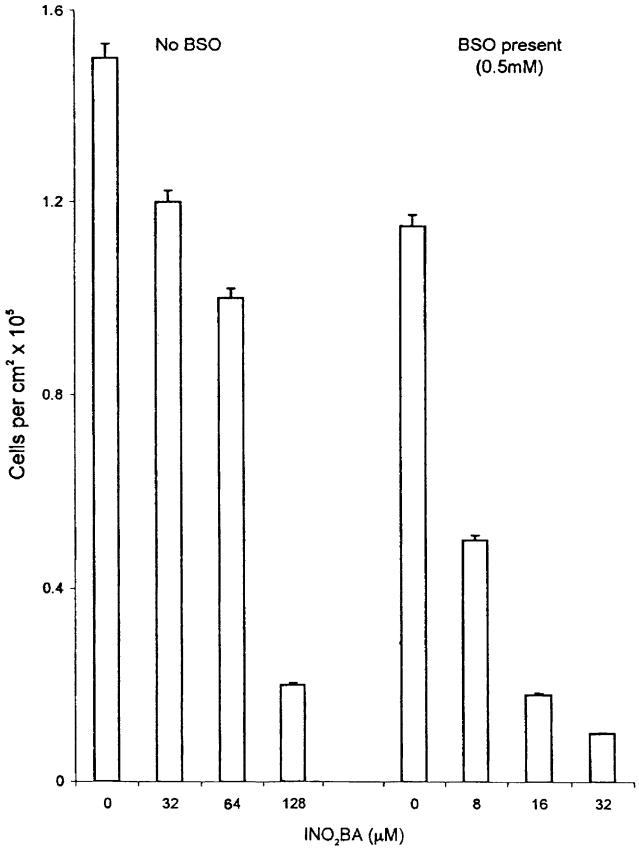

Fig. 1. Effect of INO_2BA on the growth of E-ras 20 cells in the absence and presence of BSO. E-ras 20 cells were seeded at a density of $0.16 \times 10^5/cm^2$ into 2 cm^2 tissue culture wells in the presence and absence of BSO (0.5 mM final concentration) and INO_2BA at the concentrations indicated. The drug was dissolved in regular growth medium (DMEM, 10% FBS). After 3 days of incubation (5% CO_2, 37°), medium was removed, cells were detached, and aliquots of the dispersed cell suspensions were counted in a haemocytometer. Results are the mean values of three experiments where the standard deviation was ±18%.

3.3. Uptake of [^{14}C]-INO_2BA and covalent binding of [^{14}C]-INOBA to GAPDH

When E-ras 20 cells were incubated with [^{14}C]-INO_2BA, an equilibration of extra- and intracellular drug concentration took place in 18 hr (Table 1) without BSO, a value determined experimentally. It is for this reason that an 18 hr incubation was chosen for the study of the fate of the intracellular drug. About 50% of ^{14}C-labeled drug was covalently bound to macromolecular cellular components, as determined by 10% perchloric acid (PCA) percipitable [^{14}C]. BSO greatly increased drug uptake by the removal of GSH and causing subsequent macromolecular binding of INOBA. These events may create an apparently inward oriented drug gradient resulting in an increase of intracellular drug concentration by diffusion in 18 hr (Table 1). The macromolecular component that covalently bound the labeled drug was identified by gel electrophoresis to be a protein (see Fig. 3). No DNA or RNA contained ^{14}C-label as determined by the inability of DNase or RNase to

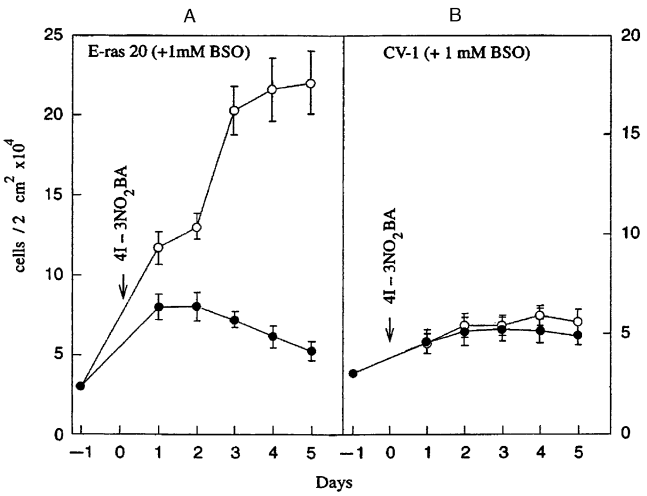

Fig. 2. Time course of cell growth of E-ras 20 and CV-1 cells. Cells were seeded into 2 cm^2 wells containing DMEM + 10% FBS + 1 mM BSO. E-ras 20: 3×10^4 cells per well; CV-1: 4×10^4 cells per well. Incubation was done at 5% CO_2, 37°. INO_2BA (4I-3NO_2BA) was added at a final concentration of 20 μM from a 10 mM stock solution in DMSO. Results are the mean ± SD of six parallel experiments. Cells were counted in a haemocytometer after their detachment. In panel A, the top curve (open circles) shows the growth rate of E-ras 20 cells without INO_2BA. When INO_2BA was added (arrow, closed circles), cell growth was inhibited. Panel B illustrates the same experiment with CV-1 cells.

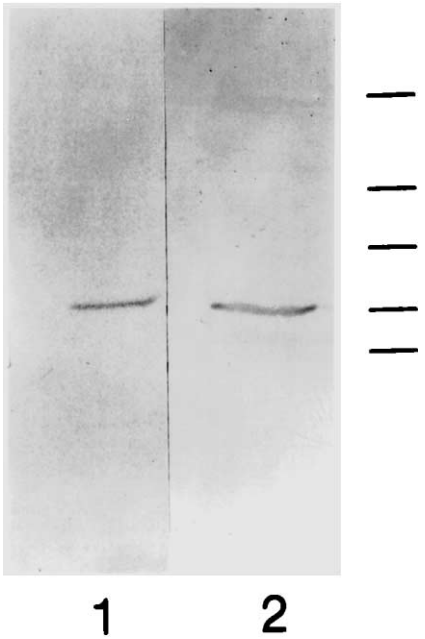

Fig. 3. Covalent binding of [^{14}C]-INOBA formed from [^{14}C]-INO_2BA to a protein of E-ras 20 cells in the presence of BSO. E-ras 20 cells (6.3×10^6) were incubated with 53 μM [^{14}C]-INO_2BA + 1.0 mM BSO for 18 hr. Cells were detached, and extracts (cf. [7]) equivalent to 2×10^5 cells were loaded onto 12% SDS-PAGE, and transblotted onto nitrocellulose; [^{14}C] was located by autoradiography. The technique of immunotransblot with GAPDH-specific antibody was the same as described earlier [25]. Lane 1: autoradiography of [^{14}C]-INOBA bound to a protein that had an apparent mass of 40 kDa. Lane 2: the same protein identified by immunotransblot with GAPDH-specific antibody. The location of the molecular weight markers (89, 67, 49, 37.5, and 34 kDa) is shown at the right margin.

solubilize the ^{14}C-label or by autoradiography on standard DNA or RNA gels (results not shown). Both the cellular uptake of [^{14}C]-INO_2BA and the covalent binding of the nitroso product to cellular protein were augmented by co-incubation with 1 mM BSO (see Table 1). The study of the cellular uptake of [^{14}C]-INO_2BA into CV-1 cells gave results very similar to those shown in Table 1 for E-ras 20 cells, with respect to equilibration of extra- and intracellular drug concentration. For example, exposure of CV-1 cells to 25–30 μM external INO_2BA yielded an intracellular drug concentration of 25–30 μM after 18 hr of equilibration. However, in sharp contrast to results shown in Table 1, pretreatment of CV-1 cells with 1 mM BSO had no influence on the quantity of intracellular acid precipitable [^{14}C] counts, demonstrating that a drastic decrease of cellular GSH content had no effect on the intracellular fate of INO_2BA in CV-1 cells (results not shown).

3.4. Identification of GAPDH as the cellular acceptor of [^{14}C]-INOBA

The isolation of the protein adduct produced by incubation of E-ras 20 cells with [^{14}C]-INO_2BA was carried out as follows. E-ras 20 cells in culture (6×10^6 cells) were incubated with 53 μM [^{14}C]-INO_2BA + 1.0 mM BSO for 18 hr at 37°, and then were detached and extracted as described previously [7]. The protein extract was concentrated, and an amount equivalent to 2×10^5 cells was loaded onto 12% SDS-PAGE, and then transblotted onto a nitrocellulose membrane; [^{14}C] was located by autoradiography (cf. [25]). Fig. 3 illustrates the results. Lane 1 shows a ^{14}C-labeled protein band with an apparent mass of 40 kDa. Lane 2: the same protein was identified by immunotransblot, using a GAPDH-specific antibody, as a subunit of GAPDH. The protein adduct was acid stable; thus, a semimercaptal structure was unlikely. The protein adduct was also stable for 2 hr at 40° at pH 7.4 even in the presence of neutral NH_2OH, but decomposed in 2 M NaOH. The ^{14}C-labeled minute amount of product after complete protein digestion with proteinase K was identified by thin-layer chromatography as the "azoxy" product obtained previously (cf. [23]). This protein-bound substance is most likely derived from the addition of a second molecule of INOBA to the initial cysteine semimercaptal adduct, which, after loss of H_2O and condensation, yields the base unstable azoxy derivative [23]. The very low quantity of protein-bound product prohibited more definitive identification. The azoxy species has been identified previously as a by-product of the reaction of INOBA and GSH [23].

3.5. Inhibition of GAPDH by the reduction product of INO_2BA

A conventional optical enzyme test (Fig. 4) illustrated a drug concentration-dependent inhibition of GAPDH after a

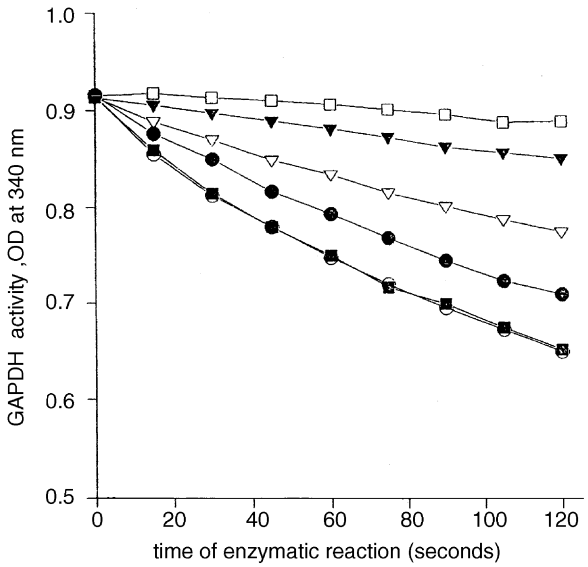

Fig. 4. Inhibitory effect of INOBA on GAPDH *in vitro*. Rabbit muscle GAPDH/GK (Sigma), obtained in a 50 μL slurry, was sedimented, and then dissolved in 50 μL of 100 mM Tris–HCl (pH 7.4). Five microliters of this solution was diluted to 1.0 mL with distilled water containing various concentrations of INOBA (stock solution in ethanol) and incubated for 12.5 min prior to the optical enzyme test, which consisted of measuring the decrease of absorbance at 340 nm. The test (in three parallel runs) was performed by initiating the reaction with 10 μL of diluted enzyme that had been preincubated with INOBA (see above). The standard deviation of the spectrophotometric reading was ±10% of the mean. The enzyme assay was that recommended by Sigma (containing phosphoglycerate kinase, ATP, and NADH at prescribed concentrations in a final volume of 1.0 mL). The decrease in absorbance at 340 nm was followed for 120 s at room temperature. Key: (□) inhibition by 100 μM INOBA; (▼) inhibition by 75 μM INOBA; (▽) inhibition by 50 μM INOBA; (●) inhibition by 25 μM INOBA; (○) and (■) no inhibitor or 100 μM INO_2BA, respectively.

12.5 min preincubation with INOBA. Prolonging preincubation with INOBA, enzyme inactivation followed a kinetics that was dependent upon both drug concentration and time of incubation (results not shown). It is also evident from Fig. 4 that 100 μM INO_2BA had no inhibitory action, as would be expected from a prodrug.

3.6. Inactivation of the glycolysis of E-ras 20 cells

The effects of prolonged incubation with 10 μM INO_2BA in the presence of 1 mM BSO are shown in Fig. 5. Inhibition of glycolysis in E-ras 20 cells was very pronounced, whereas glycolysis in CV-1 cells was not affected. These results are reminiscent of the inhibition of tumor cell growth caused by treatment with INO_2BA + BSO compared with the lack of effect on CV-1 cells (Fig. 2).

3.7. Proteolytic degradation of PARP I in E-ras 20 cells treated with INO_2BA + BSO and partial purification of the drug-induced PARP I protease

SDS-PAGE analyses of cellular proteins of E-ras 20 cells before and after combined drug treatment showed a

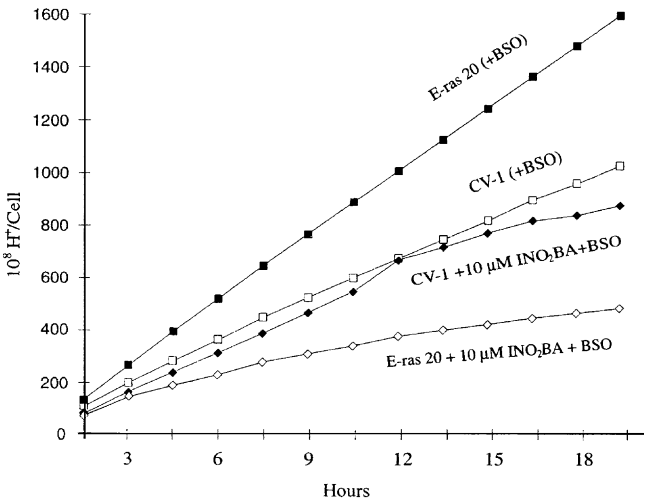

Fig. 5. Inhibition of glycolysis by INO_2BA + BSO. E-ras 20 and CV-1 cells were seeded at a density of 3×10^5/mL in 12 mm culture chambers, and treated with 10 μM INO_2BA in the presence of 1.0 mM BSO for 9 hr in an incubator at 5% CO_2, 37°. Culture medium was DMEM (Sigma) with 10% FBS added. The averaged hydrogen ion production of four control and four treated culture chambers was measured in a silicon-based microphysiometer. The standard deviation was less than ±10%.

marked decrease of the 116 kDa species of PARP I protein after drug treatment, PARP I being identified by immunotransblot (cf. [7,25]) (results not shown). Simultaneously with the decrease of the 116 kDa protein, a new band of 50 kDa mass appeared, suggesting this to be the main proteolytic degradation product of PARP I. Since the proteolytic degradation of PARP I did not take place in drug-irresponsive CV-1 cells in the presence of INO_2BA + BSO, we proceeded to isolate, partially sequence, and partially synthesize this polypeptide (see Section 2), in order to devise an isolation procedure of the proteinase from E-ras 20 cells. This seemed essential for the characterization of this drug-induced proteolysis.

Purification of the drug-induced PARP I protease was carried out as follows: 10^7 E-ras 20 cells in culture were treated with 60 μM INO_2BA and 1 mM BSO overnight at 37° and collected from cell culture dishes by dislodging cells mechanically, washing with 3 × 50 mL of PBS, and then preparing a protein extract, the details of which have been published previously [7,25]. The NaCl concentration in the extract was adjusted to 2 M by adding solid NaCl, and the cleared extract was loaded onto a Phenyl-Sepharose column (1 mL bed volume), equilibrated with the same buffer, then washed with 2 × 2 mL of loading buffer (50 mM Tris–HCl, pH 7.4, 1 mM EDTA, 7 mM 2-mercaptoethanol) followed by a stepwise gradient elution of the bound proteins by decreasing the ionic strength from 1.0 to 0.5, 0.25, and 0.0 M NaCl, each step consisting of 3 × 2 mL of eluant. PARP I proteolysis by the eluates was monitored in all fractions. The proteolytic activity (for the method of PARP I protease, see the legends to Figs. 6 and 7) was quantitatively recovered after the stepwise gradient with 3 × 3 mL of Tris (10 mM, pH 7.4; EDTA,

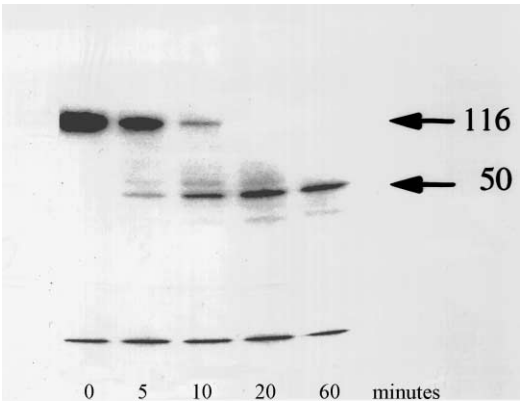

Fig. 6. Time course of degradation of PARP I by a purified (Phenyl-Sepharose stage) protease isolated from E-ras 20 cells. Five micrograms of the active protease fraction (Phenyl-Sepharose eluate, see Table 2) was incubated with 200 ng of [^{125}I]-PARP I in 200 μL of the reaction system composed of 50 mM Tris–HCl (pH 7.4), 2 mM $MgCl_2$, 2 mM $CaCl_2$, 7 mM 2-mercaptoethanol. At the time intervals shown on the ordinate, 20 μL aliquots were withdrawn, electrophoresed, and autoradiographed. Lane 1: 200 ng [^{125}I]-PARP I; lane 2: after incubation with protease for 5 min; lane 3: same as lane 2 but for 10 min; lane 4: same as lane 2 but for 20 min; lane 5: same as lane 2 but for 60 min. The arrows on the right side show the location of PARP I (116 kDa) and of the main degradation product (50 kDa) in the gel. The band at the bottom of the gel is a ^{125}I-labeled Bolton–Hunter reagent adduct of lysine.

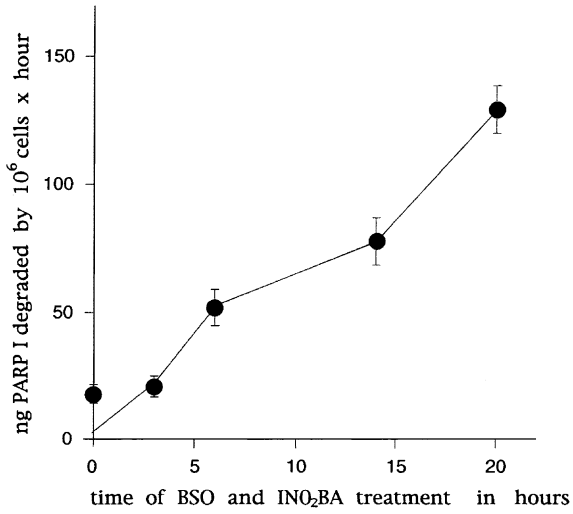

Fig. 7. Rate of PARP I poteolysis by extracts of E-ras 20 cells preincubated with INO_2BA + BSO from 0 to 18 hr. E-ras 20 cells (2×10^6) were treated with 0.8 mM BSO and 100 μM INO_2BA for the time period indicated on the abscissa. Cells were collected by scraping them into the medium, followed by centrifugation and a PBS washing step. Two million cells were lysed in 100 μL of NP-40 lysis buffer [7,25]. Sixty microliters of the extract was mixed with 180 μL of a solution containing 1.2 μg of [^{125}I]-labeled PARP I (cf. [25]) in 50 mM Tris–HCl (pH 7.4) buffer and the components listed in the legend of Fig. 6. At 0, 5, 10, 20, 40, and 60 min, 40 μL aliquots were withdrawn and analyzed by gel electrophoresis. Results (means ± SD of three experiments) were calculated in units as nanograms of PARP I degraded by 106 cells/hr.

1 mM), whereas preceding protein fractions contained no PARP I protease. The Tris fraction was concentrated to 1 mL, and 0.5 mL was reacted with a Ni^{2+}-histidine chelating column (Quiagen) that was prepared by loading the His-tagged synthetic decapeptide (5 μM) (see Section 2) onto a 0.5 mL Quiagen resin bed followed by removal of the excess peptide with 0.3 M NaCl-containing Tris buffer. This affinity column was washed with 0.5 mL fractions of the loading buffer, and the adsorbed protease was recovered in the eluted fractions 5–9. At a 100 μM concentration, the synthetic decapolypeptide (see Section 2) competitively inhibited PARP I protease activity. The results of the three purification steps are summarized in Table 2, which shows an increase in specific activity from 0.096 to 15.0 in the final product (about 160–250-fold purification). The time course of cleavage of PARP I by the purified protease is shown in Fig. 6, and the protease activity induced as a function of the time of combined drug exposure of E-ras 20 cells in Fig. 7. Nearly linear augmentation of the protease activity took place for 20 hr. It is uncertain whether or not traces of the PARP I protease were present in untreated E-ras 20 cells, but this enzyme was undetectable in CV-1 cells even after prolonged combined drug treatment, and neither INO_2BA nor BSO alone induced it in E-ras 20 cells. Among all of the commercially available protease inhibitors, only EDTA (10 mM, causing 30% inhibition), aprotinin at 1 μg/mL (inhibiting 50%), and benzamidine at 10 mM (inhibiting 25%) appeared effective in blocking the drug-induced PARP I protease. SDS-PAGE analyses of the most highly purified protease fraction gave a main protein band with an apparent mass of 60 kDa.

Table 2
Partial purification of the drug-induced PARP I protease

Purification step	Specific activity[a]	Protein	Volume (mL)	Total activity (units)[b]
Cell extract	0.096	2.5 mg/mL	5	1200
Phenyl-Sepharose	7.2	200 μg/mL	1	1440
Peptide-Sepharose	15.0	10 μg/mL	2	300

Details of purification are described in Section 3. The isolation procedure was repeated three times, and results represent mean values with ±20% SD.

[a] Specific activity: ng PARP I degraded into the specific products/μg protease/60 min.

[b] Total activity: specific activity × μg protein.

4. Discussion

Results reported here complement previously published cytotoxic mechanisms for the combined effect of INO_2BA + BSO [23]. The BSO-augmented formation of an acid stable, most probably azoxy-cysteine INOBA adduct of GAPDH provides a missing component of the previously postulated reduction mechanism of a nitro to a nitroso group in INO_2BA, followed by the covalent addition of INOBA to a reactive thiol. Ejection of Zn^{2+} from

the asymmetric Zn^{2+} finger of PARP I was previously the only evidence (cf. [23]) for a nucleophilic attack by INOBA. The dramatic selectivity of $INO_2BA + BSO$ against E-ras 20 cells, compared with non-malignant CV-1 cells (Fig. 2), is most plausibly explained by the absence of nitro-reductase activity in CV-1 cells, as demonstrated by the complete absence of augmentation of covalent protein adduct formation (from [^{14}C]-INO_2BA) in the presence of BSO. The direct binding of INOBA to GAPDH and its inactivation further support a nitro-reductase activity-dependent protein binding mechanism. In E-ras 20 cells, removal of most of the cellular nitroso-scavenging GSH by BSO caused a large increase in covalent binding of INOBA to GAPDH. This can only occur after the reduction of nitro (NO_2) to nitroso (NO) groups by putative nitro-reductases [26]. This reduction occurs anaerobically [26], yet in our cellular system aerobic conditions prevail; thus it is possible that in cancer cells there are as yet unidentified cellular nitro reducing systems that are involved in this catalysis. The BSO-stimulated covalent protein binding of INOBA, generated from INO_2BA, is an indirect cellular assay for the reduction of NO_2 to NO. Details of this system are subject to further experimental studies.

The third cellular response to $INO_2BA + BSO$ in E-ras 20 cells is the apparent induction of a PARP I protease. Caspases, which are components of apoptotic cellular pathways, are known cysteine proteases that among several other proteins also attack PARP I [27]. The apparent molecular size and the bivalent cation requirement of the $INO_2BA + BSO$-provoked PARP I protease of E-ras 20 cells argue against an identity with caspases. Furthermore, it has been demonstrated that nitrosobenzamide inactivates caspase 3 [28]; thus, if the drug that induced PARP I protease was a cysteine protease, it would have been inactivated by INOBA formed from INO_2BA. We have reported that calpain, a Ca^{2+}-dependent protease, also degrades PARP I [29]. However, the calpain-generated polypeptide products from PARP I differ from the 50 kDa polypeptide formed by the drug-induced protease in E-ras 20 cells. Whereas induction of caspases, generating a characteristic pattern of PARP I proteolysis, generally occurs during apoptosis [30], a distinct set of proteases was identified during necrotic cell death [31], and these proteases are also capable of attacking PARP I. It is of particular relevance that during $HgCl_2$-induced cell necrosis a 50 kDa polypeptide product of PARP I has been identified [31]. The coincidence of the molecular mass of this polypeptide with that described in this report (Fig. 6), providing a characteristic signature of PARP I proteolysis, may represent evidence suggesting that the $INO_2BA + BSO$-provoked protease may be related to the $HgCl_2$-induced necrosis-associated protease, and thus indicate necrotic cell death induced by $INO_2BA + BSO$. It is known that mitochondrial ATP synthesis is impaired in cancer cells [32]. Thus, powerful inhibition of glycolysis by the combined effect of $INO_2BA + BSO$ (Fig. 5) would be expected to aggravate severe ATP deficiency, a condition favoring necrotic cell death; thus, the induction of a protease characteristic of cell necrosis [31] appears reasonable. Our results support previous research that identified distinct proteolytic patterns of PARP I degradation, distinguishing apoptosis from necrosis [33].

Acknowledgments

This work was supported, in part, by Octamer Inc., and by a research grant (UC No. A-2511) from SYN-X Inc. (Canada) obtained through George Jackowski. Scientific discussions regarding developmental biology with Charles Ordahl are acknowledged with thanks.

References

[1] Yamanaka H, Penning CA, Willis EH, Wasson BD, Carson DA. Characterization of human poly(ADP-ribose) polymerase with autoantibodies. J Biol Chem 1988;263:3879–83.
[2] de Murcia G, Menissier de Murcia J, Schreiber V. Poly(ADP-ribose) polymerase: molecular biological aspects. Bioessays 1991;13:455–62.
[3] de Murcia G, Menissier de Murcia J. Poly(ADP-ribose) polymerase: a molecular nick-sensor. Trends Biochem Sci 1994;19:172–6.
[4] D'Amours D, Desnoyers S, D'Silva I, Poirier GG. Poly(ADP-rybosyl)ation reactions in the regulation of nuclear functions. Biochem J 1999;342:249–68.
[5] Shall S, de Murcia G. Poly(ADP-ribose) polymerase I: what we have learned from the deficient mouse model. Mutat Res 2000; 460:1–15.
[6] Simbulan-Rosenthal CM, Ly DH, Rosenthal DS, Konopka G, Luo R-B, Wang Z-Q, Schultz PG, Smulson ME. Misregulation of gene expression in primary fibroblasts lacking poly(ADP-ribose) polymerase. Proc Natl Acad Sci USA 2000;97:11274–9.
[7] Bauer PI, Kirsten E, Young LJT, Varadi G, Csonka E, Buki KG, Mikala G, Hu H, Comstock JA, Mendeleyev J, Hakam A, Kun E. Modification of growth related enzymatic pathways and apparent loss of tumorigenicity of a ras-transformed bovine endothelial cell line by treatment with 5-iodo-6-amino-1,2-benzopyrone (INH_2BP). Int J Oncol 1996;8:239–52.
[8] Tseng A, Lee WFM, Kirsten E, Hakam A, McLick J, Buki KG, Kun E. Prevention of tumorigenesis of oncogene-transformed rat fibroblasts with DNA-site inhibitors of poly(ADP-ribose) polymerase. Proc Natl Acad Sci USA 1987;84:1107–11.
[9] Bauer PI, Kirsten E, Varadi G, Young LJT, Hakam A, Comstock JA, Kun E. Reversion of malignant phenotype by 5-iodo-6-amino-1, 2-benzopyrone, a non-covalently binding ligand of poly(ADP-ribose) polymerase. Biochimie 1995;77:374–7.
[10] Meisterernst M, Stelzer G, Roeder RG. Poly(ADP-ribose) polymerase enhances activator-dependent transcription *in vitro*. Proc Natl Acad Sci USA 1997;94:2261–5.
[11] Oei SL, Griesenbeck J, Ziegler M, Schweiger M. A novel function of poly(ADP)ribosylation: silencing of RNA polymerase II-dependent transcription. Biochemistry 1998;37:1465–9.
[12] Bauer PI, Buki KG, Comstock JA, Kun E. Activation of topoisomerase I by poly(ADP-ribose) polymerase. Int J Mol Med 2000;5:533–40.
[13] Bauer PI, Kun E. Binding of Topo I to PARP I-antibody complex. Int J Mol Med 2000;5:153–4.

[14] Braun T, Rudnicki MA, Arnold H-H, Jaenisch R. Targeted inactivation of the muscle regulatory gene *Myf*-5 results in abnormal rib development and prenatal death. Cell 1996;71:369–82.

[15] Rice WG, Hillyer CD, Harten B, Schaeffer CA, Dorminy M, Lackey DA, Kirsten E, Mendeleyev J, Buki KG, Hakam A, Kun E. Induction of endonuclease-meditated apoptosis in tumor cells by C-nitroso substituted ligands of poly(ADP-ribose) polymerase. Proc Natl Acad Sci USA 1992;89:7703–7.

[16] Rice WG, Schaeffer CA, Graham L, Bu M, McDougal JS, Orloff SL, Villinger F, Young M, Oroszlan S, Fesen MR, Pommier Y, Mendeleyev J, Kun E. The site of antiviral action of 3-nitrosobenzamide on the infectivity process of human immunodeficiency virus in human lymphocytes. Proc Natl Acad Sci USA 1993;90:9721–4.

[17] Wondrak EM, Sakaguchi K, Rice WG, Kun E, Kimmel AR, Louis JM. Removal of zinc is required for processing of the mature nucleocapsid protein of human immunodeficiency virus, type I, by viral protease. J Biol Chem 1994;269:21948–50.

[18] Rice WR, Schaeffer CA, Harten B, Villinger F, South TL, Summers MF, Henderson LE, Bess JW, Arthur LO, McDougal JS, Orloff SL, Mendeleyev J, Kun E. Inhibition of HIV-1 infectivity by zinc-ejecting aromatic C-nitroso compounds. Nature 1003;361:473–5.

[19] Szabo C, Virag L, Cuzzocrea S, Scott GS, Hake P, O'Connor MP, Zingarelli B, Salzman A, Kun E. Protection against peroxynitrite-induced fibroblast injury and arthritis development by inhibition of poly(ADP-ribose) synthetase. Proc Natl Acad Sci USA 1998;95:3867–72.

[20] Endres M, Scott GS, Salzman AL, Kun E, Moskowitz MA, Szabo C. Protective effects of 5-iodo-6-amino-1,2-benzopyrone, an inhibitor of poly(ADP-ribose) synthetase against peroxynitrite-induced glial damage and stroke development. Eur J Pharmacol 1998;351:377–82.

[21] Szabo C, Wang HR, Bauer PI, Kirsten E, O'Connor M, Zingarelli B, Mendeleyev J, Hasko G, Vizi ES, Saltzman A, Kun E. Regulation of components of the inflammatory response by 5-iodo-6-amino-1, 2-benzopyrone, an inhibitor of poly(ADP-ribose) synthetase and pleiotropic modifier of cellular signal pathways. Int J Oncol 1997; 10:1093–101.

[22] Kun E. Poly(ADP-ribose) polymerase, a potential target for drugs: cellular regulatory role of the polymer and the polymerase protein mediated by catalytic and macromolecular colligative actions. Int J Mol Med 1998;2:131–42.

[23] Mendeleyev J, Kirsten E, Hakam A, Buki KG, Kun E. Potential chemotherapeutic activity of 4-iodo-3-nitrobenzamide. Metabolic reduction to the 3-nitroso derivative and induction of cell death in tumor cells in culture. Biochem Pharmacol 1995;50:705–14.

[24] Inveresk Research Report (4470 Redwood Highway, Suite 101, San Rafael, CA 94903): 4-iodo-3-nitrobenzamide. Investigational New Drug Application No. 56.495, Serial No. 001, Octamer Inc., Submitted to FDA, July 20 1988, approved June 1999, vol. 4.

[25] Buki KG, Bauer PI, Hakam A, Kun E. Identification of domains of poly(ADP-ribose) polymerase for protein binding and self-association. J Biol Chem 1995;270:3370–7.

[26] Mason RP, Holtzman JL. The mechanism of microsomal and mitochondrial nitroreductase. Electron spin resonance evidence for nitroaromatic free radical intermediates. Biochemistry 1975;14: 1626–32.

[27] Cohen GM. Caspases: the executioners of apoptosis. Biochem J 1997;326:1–16.

[28] Mihalik R, Bauer PI, Petak I, Krajcsi P, Marton A, Kun E, Kopper L. Interaction of cytocidal drugs and the inhibition of caspase-3 by 3-nitrosobenzamide. Int J Cancer 1999;82:875–9.

[29] Buki KG, Bauer PI, Kun E. Isolation and identification of a proteinase from calf thymus that cleaves poly(ADP-ribose) polymerase and histone H1. Biochim Biophys Acta 1997;1338:100–6.

[30] Hengartner MO. The biochemistry of apoptosis. Nature 2000;407: 770–6.

[31] Casiano CA, Ochs RL, Eng MT. Distinct cleavage products of nuclear proteins in apoptosis and necrosis revealed by autoantibody probes. Cell Death Differ 1998;5:183–90.

[32] Singer S, Souza K, Thilly WG. Pyruvate utilization, phosphocholine and adenosine triphosphate (ATP) are markers of human breast tumor progression. A ^{31}P- and ^{31}C-nuclear magnetic resonance (NMR) spectroscopic study. Cancer Res 1995;55:5140–5.

[33] Shah GM, Shah GS, Poirier GG. Different cleavage patterns for poly(ADP-ribose) polymerase during necrosis and apoptosis in HL-60 cells. Biochem Biophys Res Commun 1996;229:838–44.